羌塘地体南缘改则格列戈阿尔辉长岩锆石U-Pb年代学、地球化学及地质意义

陶刚[1)],李智武[1,2)],朱利东[1)],张玉修[3)],杨文光[1)],陈顺[4)],解龙[1)],杨珍[1)],和源[1)],刘和[1)],李超[1)]

1)成都理工大学沉积地质研究院,成都,610059;

2)油气藏地质及开发工程国家重点实验室,成都,610059;

3)中国科学院大学地球科学学院,北京,100049;4)四川核工业地质局282大队,四川德阳,618000

内容提要: 改则格列戈阿尔辉长岩侵入于羌塘地体南缘木嘎岗日群,为研究班公湖—怒江缝合带在改则地区的演化提供新的强有力的约束。本文对辉长岩进行了LA-ICP-MS锆石U-Pb定年,结果显示格列戈阿尔辉长岩锆石U-Pb年龄加权平均值为122.9±1.6Ma,表明该辉长岩体形成时代为早白垩世中晚期。岩石地球化学研究表明,该区早白垩世辉长岩具有高Al_2O_3(15.39%~16.83%)、低TiO_2(0.78%~0.92%)、贫P_2O_5(0.09%~0.17%)和低碱(Na_2O+K_2O=3.93%~4.41%)的特点。稀土元素总量(ΣREE)为63.37×10^{-6}~73.76×10^{-6},平均为68.84×10^{-6},稀土元素配分曲线呈右倾型,$(La/Yb)_N$介于2.43~3.09之间,δEu=0.89~1.03,表现弱的负铕异常,具有明显的轻稀土富集,重稀土亏损特征。岩石微量元素总体上富集大离子亲石元素(LILE)Rb、Ba、Th、U等,显著亏损高场强元素(HFES)Nb、Ta、P、Ti等,Nb/Ta、Zr/Hf比值接近或略低于原始地幔组成。根据地球化学特征和微量元素构造判别图结果表明,该辉长岩源区为被俯冲改造的岩石圈地幔源岩浆,岩浆在演化过程中遭受了上地壳物质的同化混染,并经历一定程度的结晶分异作用。格列戈阿尔辉长岩形成于班公湖—怒江洋向北俯冲构造环境下的岛弧环境,表明至少在122.9±1.6Ma期间班公—怒江洋盆正在向北俯冲。结合区域资料,研究区班公—怒江洋盆闭合时间应介于110~85Ma之间。

关键词: 辉长岩;锆石U-Pb定年;地球化学;岛弧环境;班公湖—怒江缝合带;羌塘

班公湖—怒江缝合带夹持于羌塘地块与拉萨地块之间,是青藏高原上规模最大的缝合带之一,也是青藏高原上特征鲜明的近东西向延伸的构造带(图1a)。前人对班怒缝合带进行过大量的研究工作(Kapp et al.,2003,潘桂堂等,2004,曲晓明等,2006,2009,张玉修等,2007,Zhang Kaijun et al.,2007,2008,2012,赵元艺等,2010,杜德道等,2011,ZhangYuxiu et al.,2015,付佳俊等,2015,秦川等,2015),但是由于班公湖—怒江缝合带本身的构造复杂性,随着时间推移和研究工作的开展,对于该缝合带中一些基本特征存在较大争议,尤其是在班公湖—改则段,前人对于班公湖—怒江缝合带俯冲极性和闭合时限两个基础问题就一直制约着我们对青藏高原地质背景和演化历史的研究。如:围绕着洋壳的俯冲方向,有人认为向北向羌塘地体下俯冲(Kapp et al.,2003,张玉修等,2007,付佳俊等,2015),也有学者认为是朝南向拉萨地体之下俯冲(朱弟成等,2006),同时也有学者认为班怒洋盆是双向俯冲(杜德道等,2011)。

班公湖—怒江缝合带闭合具有穿时性,总体上为东早西晚,在改则—东巧段最晚(付佳俊等,2015)。其中在青藏高原中部的永珠蛇绿岩和阿索蛇绿岩年龄为132~108Ma,代表洋盆闭合时间为晚白垩世(Zhang Kaijun et al.,2012);改则—尼玛段构造、沉积特征表明碰撞时间为早白垩世(Kapp et al.,2005)。

本文以羌塘地块南缘改则地区格列戈阿尔辉长岩为研究对象(图1),通过对该辉长岩体的岩石学、

注:本文为中国地质项目(编号:1212011086065,12120113033004)和国家自然科学基金项目(编号:41472209,41002055)以及高等学校博士学科点专项科研基金(编号:20125122110010)的成果。

收稿日期:2016-01-20;改回日期:2016-08-22;责任编辑:章雨旭。Doi:10.16509/j.georeview.2016.05.005

作者简介:陶刚,男,1988年生。博士研究生,主要从事区域地质、地球化学研究。Email:taogang0428@163.com。通讯作者:李智武,男,1976年生。教授,从事区域构造地质和油气地质研究。Email:lizhiwu06@cdut.cn。

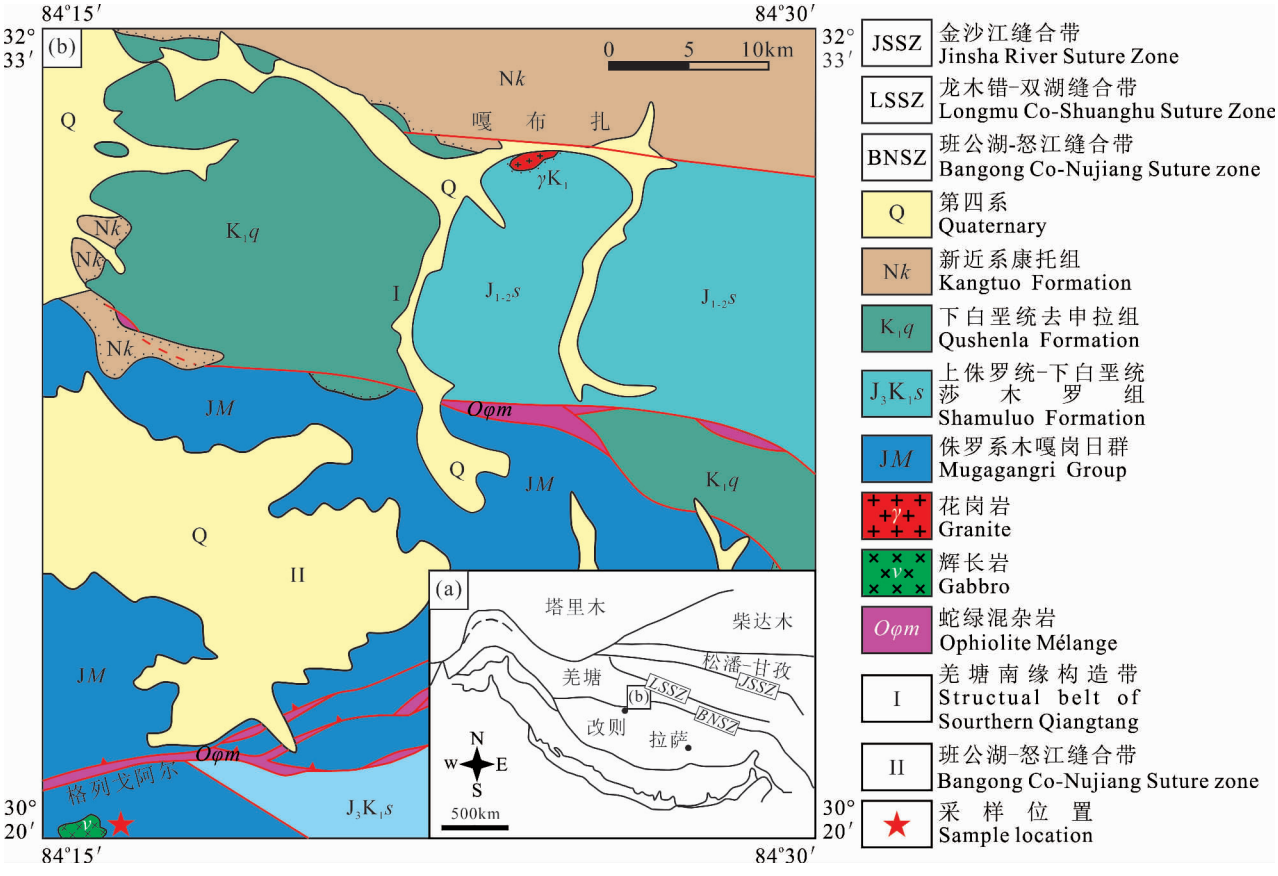


图 1 青藏高原构造单元图(a)及改则格列戈阿尔地质图(b)

Fig. 1 Tectonic subdivision of the Qinghai—Xizang(Tibet) Plateau (a) and simplified geological map of the Gelegear area, Gaize (b)

BNSZ—班公湖—怒江缝合带;LSSN—龙木错—双湖缝合带;JSSZ 金沙江缝合带。1—蛇绿岩单元;2—康托组;3—去申拉组;4—莎木罗组;5—色哇组;6—木嘎岗日群;7—花岗岩;8—辉长岩;9—羌塘南缘构造带;10—班公湖—怒江缝合带;11—洞错蛇绿混杂岩带;12—木嘎岗日群构造单元;13—单斜构造单元;14—断层;15—采样位置

BNSZ—Bangong—Nujiang Suture Zone; LSSN— Longmucuo—Shuanghu Suture Zone; JSSZ—Jinshajiang Suture Zone. 1—Ophiolite Unit; 2—Kangtuo Formation; 3—Qushenla Formation; 4—Shamuluo Formation; 5— Sewa Formation; 6— Mugagangri Group; 7—Granite; 8—Gabbro; 9—Structual belt of Sourthern Qiangtang; 10—Bangong—Nujiang Suture; 11—Ophiolite Melange Belt of Dongcuo; 12—Tectonic Unit of Mugagangri Group; 13—Tectonic Unit of Monoclinie; 14—Fault; 15—Sample Site

LA-ICP-MS 锆石 U-Pb 同位素年龄及地球化学研究,结合区域研究资料,揭示其形成时代、岩石成因及其形成的大地构造背景,探讨改则地区班公湖—怒江缝合带消减—闭合演化过程。

1 地质背景

研究区位于羌塘地块南缘改则地区,由北向南分别横跨羌塘地块南缘陆缘次级构造带(I)和班公湖—怒江缝合带(II)两个构造单元。其中,羌塘南缘构造带主要由色哇组($J_{1-2}s$)、去申拉组(K_1q)、康托组(Nk)及唢呐湖组(Ns)构成。色哇组主要以细碎屑岩为主;去申拉组为一套完整火山—沉积建造;康托组以代表山间盆地磨拉石沉积的紫红色砂砾岩为主,唢呐湖组则为一套河流碎屑岩夹湖相碳酸盐岩沉积。班怒带主要由洞错蛇绿混杂岩带($\text{Ⅱ}_{1,3}$)、木嘎岗日群($\text{Ⅱ}_{2,4}$)和单斜构造(Ⅱ_5)3 个次级构造单元构成(图 1b)。蛇绿混杂岩带岩石组分主要有变质橄榄岩、堆积岩、辉绿岩、玄武岩等;木嘎岗日群主要为灰黑色板岩—砂岩夹有玄武岩—安山岩岩块;而单斜构造则由沙木罗组(J_3K_1s)碎屑岩夹碳酸盐岩构成。

2 岩体地质及岩石学特征

格列戈阿尔辉长岩体位于南羌塘地体南缘,改则县城北东 10 km 处,GPS 坐标位置:N30°20′30″,E84°15′41″。岩体在平面上呈不规则的椭圆状,呈

南北向展布。岩体露头较好,风化面为灰绿至灰白色,新鲜颜色为灰色至深灰色,边缘可见烘烤边(图 2a,b),矿物为中粗粒结构,与周边木嘎岗日群岩块形成侵入接触关系(图 2c,d)。辉长岩主要由斜长石(40% ~45%)、辉石(30% ~40%)、角闪石(5% ~10%)、磷灰石(2% ~5%)及榍石、锆石和磁铁矿等副矿物组成,镜下观测辉长岩样品具典型的辉长结构(图 2e,f,g,h),矿物颗粒一般为 2 ~4mm。其中,斜长石多为板条状—宽板状,发育卡钠复合双晶、钠长石双晶,有弱的粘土化、绢云母化现象;辉石多为半自形粒状,与斜长石镶嵌分布,自形程度相当,颗粒边缘可见局部发生次闪石化;角闪石呈自形状,内部常包含辉石颗粒(图 2g,h);黑云母为细片状,常沿辉石颗粒边缘分布(图 2e);磁铁矿为不规则团粒状,沿斜长石解理缝分布(图 2f)。用于本文研究的 7 件辉长岩样品采自于西藏改则格列戈阿尔地区,样品尽可能地覆盖整个辉长岩体,采样过程中尽量选取新鲜无风化、纯净无脉的岩石样品,采样位置见图 1。

3　LA-ICP-MS 锆石 U-Pb 同位素测定

为了获取格列戈阿尔辉长岩体形成时代,采用 LA-ICP-MS 法对该岩体中岩浆锆石进行 U-Pb 同位素测年分析,在岩体中南部采集新鲜无蚀变的辉长岩样品 5kg,采样中避开节理发育和蚀变严重地段。

3.1　测试方法

锆石分选工作在河北区域地质调查研究所完成,测试样品经人工破碎后,用常规重液和磁选方法分选出锆石,在双目镜下挑选。将待测样品的锆石颗粒、标准锆石 M257 和 TEM 置于环氧树脂制靶,然后研磨至一半,用于透射光、反射光、阴极发光(CL)和 U-Pb 定年分析。U-Pb 同位素定年分析在中国地质科学院矿产资源研究所国土资源部成矿作用与资源评价重点实验室完成,所用仪器为 FinniganNeptune 型 MC-ICP-MS 及与之配套的 Newwave UP 213 激光剥蚀系统。激光剥蚀所用束斑直径为 25 μm,频率为 10 Hz,能量密度约为 2.5 J/cm^2,以 He 为载气。LA-ICP-MS 激光剥蚀采样采用单点剥蚀的方式,锆石 U-Pb 测年以锆石 GJ-1 为外标进行校正。测试过程中每测定 10 个点重复测定两个标样锆石 GJ-1 对样品进行校正,并测量一个锆石标样,观察仪器的状态和测试的重现性。数据处理采用 ICPMSDataCal 程序,测量过程中绝大多数分析点$^{206}Pb/^{204}Pb > 1000$,未进行普通铅校正,^{204}Pb 由离子计数器检测,^{204}Pb 含量异常高的分析点可能受包体等普通 Pb 的影响,这些点在计算时剔除。锆石标准的重现性在 1%(2σ)左右。所测数据应用 Isoplot 3.0 程序进行数据处理,所得出的同位素比值和年龄的误差均在 1σ 水平(侯可军等,2009,秦川等,2015)。

3.2　分析结果

格列戈阿尔辉长岩中代表性锆石阴极发光 CL 图像及分析点见图 3,锆石 U-Pb 分析结果见表 1。格列戈阿尔辉长岩体中锆石形态呈长柱状或短柱状,自形程度较高(图 3),锆石长宽比在 2∶1 ~4∶1 之间,CL 图像显示锆石呈灰色,部分呈深灰色,可能与锆石的 REE 或 U、Th 含量较多有关,Th/U 比值介于 0.53 ~3.14,大于 0.1,指示其为岩浆结晶产物。锆石内部结构具有较宽的结晶环带,推测其锆石晶体生长时温度较高,微量元素扩散快所致,也表明锆石为岩浆成因。

从锆石 U-Pb 协和图 4 看出,分析点均位于谐和线上或附近。12 个测点$^{206}Pb/^{238}U$ 年龄相对集中,变化在 121 ~154Ma 之间。各测点在一致曲线上形成一个年龄聚集区(图 4),其加权平均年龄为 122.9 ±1.6Ma(MSWD = 0.08),表明格列戈阿尔辉长岩岩体侵位时代为早白垩世中晚期。

4　辉长岩地球化学特征

4.1　分析方法

主量元素在中南大学地球科学与信息物理实验中心完成,采用粉末压片法完成分析测试,所用仪器为 ZSX Primus II 型 X 射线荧光光谱仪,实验分析精度优于 1%。微量元素由中国科学院青藏高原研究所实验测试中心分析,实验测试仪器使用美国 Thermo 公司生产的 X Series 电感耦合等离子体质谱仪。测试时首先采用酸溶法对样品进行预处理,然后再利用 ICP-MS 法测定,分析精度优于 5%。

4.2　主量元素

7 件格列戈阿尔辉长岩样品全岩地化分析数据见表 2。样品 SiO_2 含量变化范围较小,在 50.67% ~53.28% 之间,平均值为 51.89%,Al_2O_3 含量较高,在 15.39% ~16.83% 之间,平均值为 16.05%,具有消减带岩石特征(张旗和周国庆,2001);CaO 含量在 7.83% ~9.09% 之间;MgO 含量变化在 3.20% ~3.53% 之间;$Mg^{\#}$ 指数为 45.02 ~47.71,平均值为 46.19,低于基性原生岩浆的 Mg#值范围(68


v
JM
(a)
(b)
Nikon
(c)
(d)
Pl
Pl
Py
(e)
1000μm
Pl
Py
Py
Pl
(f)
1000μm
Py
Pl
Amp
(g)
1000μm
Py
Pl
Amp
Mt
Pl
(h)
1000μm

图 2 改则格列戈阿尔辉长岩野外露头及显微照片

Fig. 2 Fields and microp hotographs of the Gelegeargabbro in Gaize

(a)辉长岩体与木嘎岗日群界线宏观照;(b)辉长岩与木嘎岗日群岩块侵入接触关系;(c)、(d)辉长岩野外露头照;(e)、(f)辉长岩中典型辉长结构,辉石颗粒边缘局部发生次闪石化;(g)、(h)中—粗粒辉长结构,斜长石有弱的绢云母化,普通角闪石内部常包含辉石颗粒。Py—辉石,Pl—斜长石,Amp—角闪石,Mt—磁铁矿

(a) The photo of the boundary line between the Gabbro and the Mugagangri Group; (b) the intrusive contact relationship between the Gabbro and the rock block of the Mugagangri Group; (c), (d) The outcrops of the Gabbro; (e), (f) The gabbro texture, the granular edge of pyroxene developed ouralite; (g), (h) medium to coarse grained gabbro texture, plagioclase developed sericitization, pyroxene granules in amphibole. Py—Pyroxene; Pl—Plagioclase; Amp—Amphibole; Mt—Magnetite

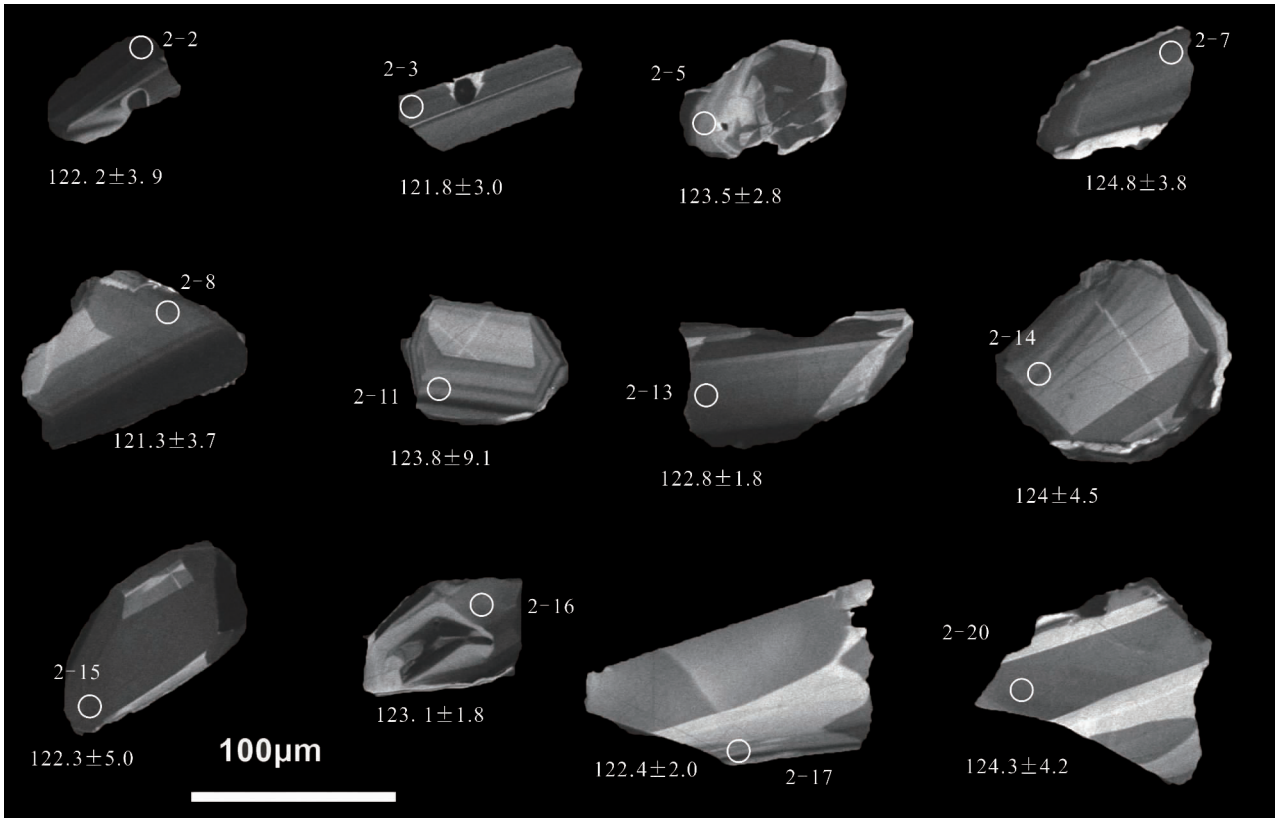


图 3 改则格列戈阿尔辉长岩锆石阴极发光照片

Fig. 3 Cathodoluminescence(CL) images of zircon from the Gelegear gabbro in Gaize

~75),表明岩浆经历了一定程度的分离结晶作用;TiO_2 含量为 0.78% ~0.92%,平均值为 0.84%,含量低于大洋拉斑玄武岩的 2.63% 和大陆溢流拉斑玄武岩的 TiO_2 的 1.0%(Wilson,1989),但很接近于岛弧拉斑玄武岩中 TiO_2 含量 0.8%(Jakes et al.,1972,田亚洲等,2014),反映源区可能与俯冲环境有关;Na_2O 含量为 3.59% ~3.85%,K_2O 含量为 0.26% ~0.67%,全碱($Na_2O + K_2O$)为 3.93% ~4.41%,$Na_2O/K_2O > 1$,在 SiO_2—K_2O 图上(图 5a),岩石落在低钾拉斑系列范围内。总体上看,格列戈阿尔辉长岩体具有高 Al 低 Ti、贫 P_2O_5(0.09% ~0.17%)和低碱的特点。根据 TAS 分类图,格列戈阿尔辉长岩体全部点落在亚碱性辉长岩范围内(图 5b)。由 Harker 图解(图 6)可知,SiO_2 与 Al_2O_3、CaO、TiO_2、MgO、Fe_2O_3 具有一定的相关性,表明结晶分异在岩浆演化过程中具有重要作用。

4.3　稀土和微量元素

格列戈阿尔辉长岩 7 件样品稀土元素总量 ΣREE 为 63.37×10^{-6} ~ 73.76×10^{-6},平均为 68.84×10^{-6},轻、重稀土元素比值 ΣLREE/ΣHREE = 2.99 ~3.69,$(La/Yb)_N$ = 2.43 ~3.09,属轻稀土富集型。7 件样品稀土元素球粒陨石标准化配分模式十分相

表 1 改则格列戈阿尔辉长岩 LA-ICP-MS 锆石 U-Pb 测年数据

Table 1 LA-ICP-MS Zircons U-Pb data of the Gelegear gabbro in Gaize

测点号	元素含量及比值				同位素比值						同位素年龄(Ma)				
	Pb	Th	U	Th/U	$\frac{n(^{206}Pb)}{n(^{238}U)}$		$\frac{n(^{207}Pb)}{n(^{235}U)}$		$\frac{n(^{207}Pb)}{n(^{206}Pb)}$		$\frac{n(^{206}Pb)}{n(^{238}U)}$		$\frac{n(^{207}Pb)}{n(^{235}U)}$		谐和度(%)
	$\times 10^{-6}$				测值	±1σ	测值	±1σ	测值	±1σ	测值	±1σ	测值	±1σ	
2-1	288.23	288	643	0.45	0.01990	0.00027	0.16842	0.00505	0.06148	0.00185	127.0	4	158.0	4	78
2-2	709.55	710	1490	0.48	0.01914	0.00061	0.13477	0.00281	0.05107	0.00060	122.2	3	128.4	3	95
2-3	184.77	185	355	0.52	0.01907	0.00047	0.13010	0.00397	0.04958	0.00127	121.8	4	124.2	4	98
2-4	1514.57	1515	207	7.32	0.19302	0.00196	2.08883	0.02240	0.07846	0.00027	1137.7	7	1145.1	7	99
2-5	481.55	482	463	1.04	0.01934	0.00044	0.13329	0.00382	0.05002	0.00093	123.5	3	127.1	3	97
2-6	389.35	389	243	1.60	0.01930	0.00067	0.15351	0.00722	0.05768	0.00180	123.2	6	145.0	6	83
2-7	150.21	150	196	0.77	0.01954	0.00059	0.13785	0.00956	0.05104	0.00281	124.8	9	131.1	9	95
2-8	75.89	76	139	0.54	0.01900	0.00059	0.12827	0.00308	0.04917	0.00142	121.3	3	122.5	3	99
2-9	359.63	360	220	1.63	0.01948	0.00052	0.17529	0.01170	0.06467	0.00311	124.4	10	164.0	10	72
2-10	441.17	441	18	24.6	0.14599	0.00253	1.40616	0.02882	0.06983	0.00079	878.4	12	891.5	12	98
2-11	6.59	7	112	0.06	0.01939	0.00145	0.14307	0.02603	0.05232	0.00596	123.8	23	135.8	23	90
2-12	2.73	3	41	0.07	0.02427	0.00121	0.17967	0.01695	0.05345	0.00353	154.6	15	167.8	15	91
2-13	671.72	672	459	1.46	0.01924	0.00029	0.12863	0.00200	0.04860	0.00056	122.8	2	122.9	2	99
2-14	65.30	65	79	0.83	0.01942	0.00072	0.13814	0.00926	0.05141	0.00254	124.0	8	131.4	8	94
2-15	310.77	311	311	1.00	0.01915	0.00079	0.13327	0.00697	0.05048	0.00167	122.3	6	127.0	6	96
2-16	123.99	124	146	0.85	0.01928	0.00029	0.13814	0.00461	0.05192	0.00152	123.1	4	131.4	4	93
2-17	141.29	141	28	5.04	0.01917	0.00032	0.14002	0.00558	0.05317	0.00214	122.4	5	133.1	5	91
2-18	173.49	173	158	1.10	0.01770	0.00108	0.20694	0.01868	0.08463	0.00252	113.1	16	191.0	16	48
2-19	5.41	5	26	0.21	0.01873	0.00049	0.17913	0.01587	0.06943	0.00613	119.6	14	167.3	14	66
2-20	30.72	31	82	0.37	0.01947	0.00066	0.12976	0.01047	0.04811	0.00231	124.3	9	123.9	9	99

注:表中测点号前省去了“D1154-N1-”。

似,呈右倾曲线,无较大异常变化,表明来自同源区(图 7a),总体反映轻稀土元素分馏较好,重稀土元素分馏较差。曲线模式与地幔岩浆型稀土元素曲线模式大致相似,说明岩浆来源与地幔岩浆有密切关系(左祖发等,2015)。$\delta_{Eu}=0.89\sim1.03$,$\delta_{Ce}=0.98\sim1.01$,Eu 和 Ce 表现弱的负异常。

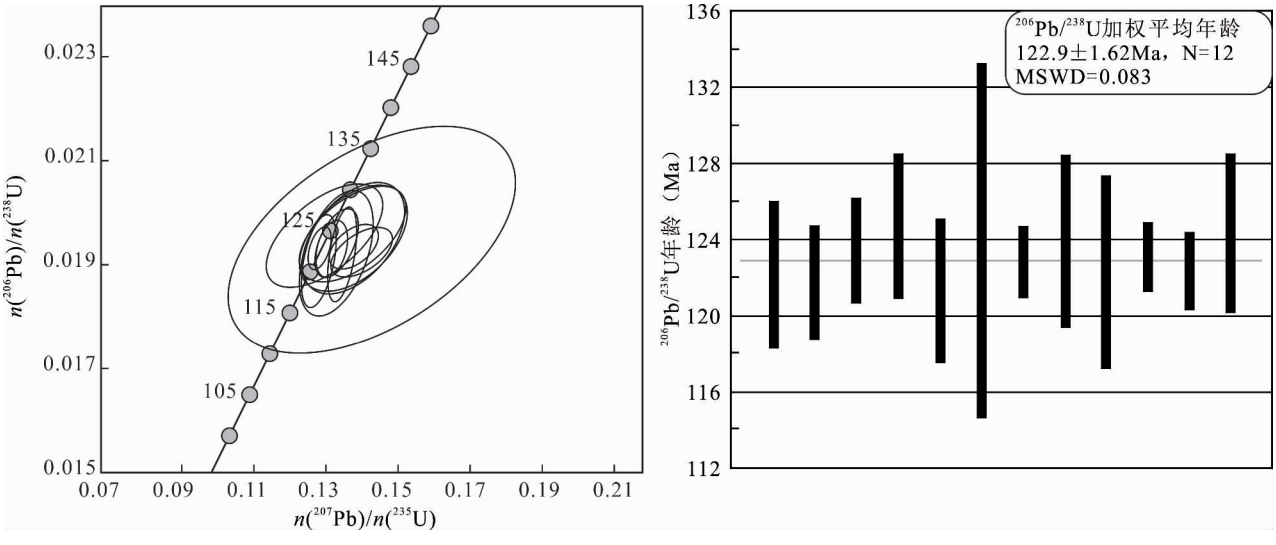


图 4 改则格列戈阿尔辉长岩锆石 U-Pb 谐和图和加权年龄平均值

Fig. 4 Concordia plot and weighted U-Pb age mean of the zircon from the Gabbro in Gelegeaer, Gaize

表 2 改则格列戈阿尔辉长岩主量元素(%)和微量元素(μg/g)的地球化学分析数据

Table 2 Major(%) and trace elements(μg/g) compositions of the Gelegear gabbro in Gaize

岩石名称	辉长岩						
样品编号	P36-9H1	P36-9H2	P36-11H1	P36-11H2	P36-12H1	P36-16H1	P36-16H4
SiO_2	51.86	51.66	51.60	53.28	52.59	50.67	51.59
TiO_2	0.84	0.87	0.81	0.80	0.78	0.92	0.89
Al_2O_3	16.09	16.07	15.73	15.59	15.39	16.83	16.67
Fe_2O_3	1.10	1.10	1.08	1.05	1.08	1.13	1.09
FeO	6.22	6.26	6.12	5.95	6.14	6.38	6.17
MnO	0.24	0.20	0.22	0.21	0.22	0.20	0.22
MgO	3.53	3.23	3.36	3.31	3.20	3.25	3.22
CaO	8.94	9.09	8.34	8.06	7.83	8.81	8.05
Na_2O	3.78	3.85	3.82	3.59	3.70	3.64	3.74
K_2O	0.39	0.26	0.32	0.34	0.33	0.44	0.67
P_2O_5	0.15	0.17	0.15	0.09	0.12	0.16	0.17
LOI	5.65	5.83	6.48	5.13	7.06	6.23	6.17
Total	98.79	98.59	98.02	98.41	98.43	98.64	98.64
Rb	15.34	9.36	12.04	11.64	8.60	11.65	20.04
Sr	381.30	376.90	332.30	305.10	407.50	368.40	358.20
Ba	146.70	121.30	150.10	154.00	174.70	153.70	192.80
Th	1.77	1.05	1.89	1.82	1.37	2.13	2.77
U	0.41	0.32	0.40	0.43	0.36	0.60	0.53
Nb	4.29	3.78	4.17	4.02	3.47	3.95	4.16
Ta	0.26	0.23	0.24	0.24	0.18	0.23	0.27
Zr	79.04	84.19	59.27	56.23	72.06	57.33	73.04
Hf	2.21	2.28	1.87	1.82	2.37	1.82	2.28
Co	26.62	25.70	25.73	23.77	23.64	25.75	24.05
Ni	12.16	11.20	10.48	15.51	10.82	11.49	9.29
Cr	20.10	28.95	19.37	24.47	16.66	21.28	16.50
V	259.40	276.50	254.80	243.40	220.60	284.40	271.30
Sc	27.33	27.02	28.09	27.48	24.78	31.52	26.24
Cs	0.44	0.24	0.76	0.49	0.33	0.43	0.44
Ga	19.48	19.99	19.54	18.77	17.15	20.04	19.99
Cu	31.82	45.07	44.55	34.29	33.41	50.21	47.82
Pb	3.35	2.92	3.24	3.16	3.06	2.78	3.04
Zn	90.35	86.10	86.50	79.46	83.85	84.57	85.69
La	9.76	9.33	10.57	8.93	9.75	10.21	11.32
Ce	21.44	20.89	23.20	20.12	22.63	22.66	24.08
Pr	2.70	2.81	3.10	2.74	3.02	3.02	3.17
Nd	12.00	13.23	14.04	12.58	13.29	13.82	14.09
Sm	2.91	3.43	3.70	3.27	3.22	3.51	3.54
Eu	1.06	1.18	1.16	1.08	0.98	1.19	1.18
Gd	3.41	4.07	4.31	3.98	3.70	4.18	4.15
Tb	0.57	0.68	0.73	0.69	0.65	0.74	0.68
Dy	3.62	4.48	4.74	4.51	4.18	4.61	4.43
Ho	0.76	0.96	0.98	0.94	0.86	0.95	0.94
Er	2.22	2.73	2.88	2.73	2.56	2.75	2.73
Tm	0.33	0.40	0.42	0.40	0.39	0.40	0.40
Yb	2.26	2.75	2.85	2.65	2.66	2.60	2.64
Lu	0.34	0.40	0.42	0.40	0.40	0.39	0.40
Y	20.84	25.93	26.91	25.30	24.12	25.72	25.11
Ti	5930.00	5974.00	5866.00	5455.00	5016.00	6589.00	6522.00
ΣREE	63.37	67.33	73.10	65.02	68.30	71.02	73.76
LREE/HREE	3.69	3.09	3.22	2.99	3.43	3.28	3.50
$(La/Yb)_N$	3.09	2.43	2.66	2.42	2.63	2.82	3.07
δEu	1.03	0.96	0.89	0.91	0.87	0.95	0.94
δCe	1.01	0.99	0.98	0.99	1.01	0.99	0.97

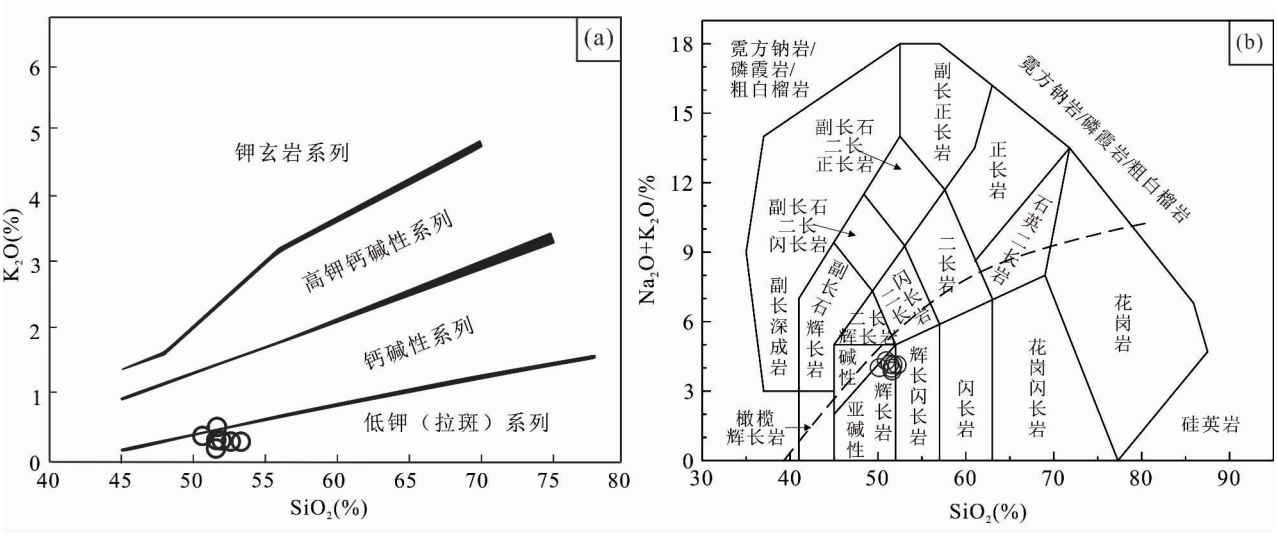


图 5 改则格列戈阿尔辉长岩 SiO_2—K_2O 图解(a)和 TAS 图解(b)

Fig. 5 SiO_2—K_2O diagram(a) and TAS diagram(b) of the Gelegear gabbro in Gaize

样品微量元素分析结果见表 2,辉长岩原始地幔标准化微量元素蛛网图(图 7b)图中显示,重稀土配分曲线相对平坦,轻稀土配分曲线富集型,具体表现为 Rb、Ba、Th、U 等大离子亲石元素(LILE)明显富集,高场强元素(HFES)中的 Nb、Ta、P、Ti 等显著亏损,曲线整体上呈右倾三隆起典型的火山弧玄武岩曲线类型,均为板块汇聚边缘岩浆岩特征(姜常义等,2001);另一方面,微量元素整体上具有相似的标准化曲线形式,且 Nb/Ta 比值在 15.28 ~ 18.96 之间,Zr/Hf 比值在 30.37 ~ 36.97 之间,接近或略低于原始地幔组成,又显示了同源岩浆演化分异特征(Nb/Ta = 17;Zr/Hf = 36;Sun et al. ,1989)。

5 讨论

5.1 格列戈阿尔辉长岩形成时代及其构造意义

锆石 CL 图像显示(图 3),来自格列戈阿尔辉长岩的锆石粒径较小,阴极发光偏弱,但是环带构造明显,较高的 Th/U 比值,属于典型的岩浆成因锆石。14 个测点的 $^{206}Pb/^{238}U$ 年龄加权平均值为 122.9 ± 1.6Ma(MSWD = 0.08),表明岩体形成时代为早白垩世中晚期。

格列戈阿尔辉长岩体具有相似的地球化学特征,岩石稀土元素分布形式呈轻稀土元素相对比重稀土元素富集,岩石富集大离子亲石元素(LILE),显著亏损高场强元素(Nb、Ta),与典型的岛弧型火山岩地球化学特征一致。正确使用火成岩图解对于区域构造环境判别有着重要的作用(邓晋福等,2015a),从构造环境判别图 8 可见,格列戈阿尔辉长岩样品均落在岛弧环境,格列戈阿尔辉长岩体最有可能是班公—怒江洋向北俯冲构造环境下的岛弧岩浆岩。区域上该时期岛弧特征岩浆岩也有出露:改则西部的多不杂富金斑岩铜矿中 121.6 ± 1.9Ma 的花岗闪长斑岩(李金祥等,2008);多龙斑岩铜矿区的 121 ~ 106Ma 的玄武安山岩和花岗闪长岩等(Li Jinxiang et al. ,2011)。综上表明格列戈阿尔辉长岩(123 ± 2Ma)是形成于俯冲环境的岛弧岩浆岩,反映研究区班公湖—怒江洋在早白垩世还在继续发生俯冲,其闭合时间应晚于早白垩世中期。

5.2 岩浆源区和岩石成因

与下地壳部分熔融有关的岩浆产物 $Mg^{\#}$ 一般小于 40(Atherton et al. ,1993),而格列戈阿尔辉长岩 $Mg^{\#}$ 变化于 45.02 ~ 47.71,平均值 46.19,表明其原生岩浆不可能为下地壳镁铁质岩石部分熔融形成,辉长岩的 Ta/Yb 比值均 < 0.12,且 Ni、Cr、V 高和低 Rb 均说明岩浆来源于地幔。通常,幔源岩浆侵入地壳过程中会不同程度受到地壳物质的影响,如果幔源岩浆在上升过程中有地壳物质的加入,往往会会使得岩石组分中大离子亲石元素含量增加,同时会使 La/Nb、Zr/Nb 比值升高,Ce/Pb 比值降低,而且总分配系数相同或相近,不受分离结晶和部分熔融程度影响,因此,元素之间含量比值及元素比值之间相关关系(如 Ce/Pb、Nb/U、La/Yb—Th/Ta、Ta/Yb—Th/Yb)可以准确验证同化混染作用是否存在(姜常义等,2015)。地壳中 Ce/Pb 比值 < 15,而典

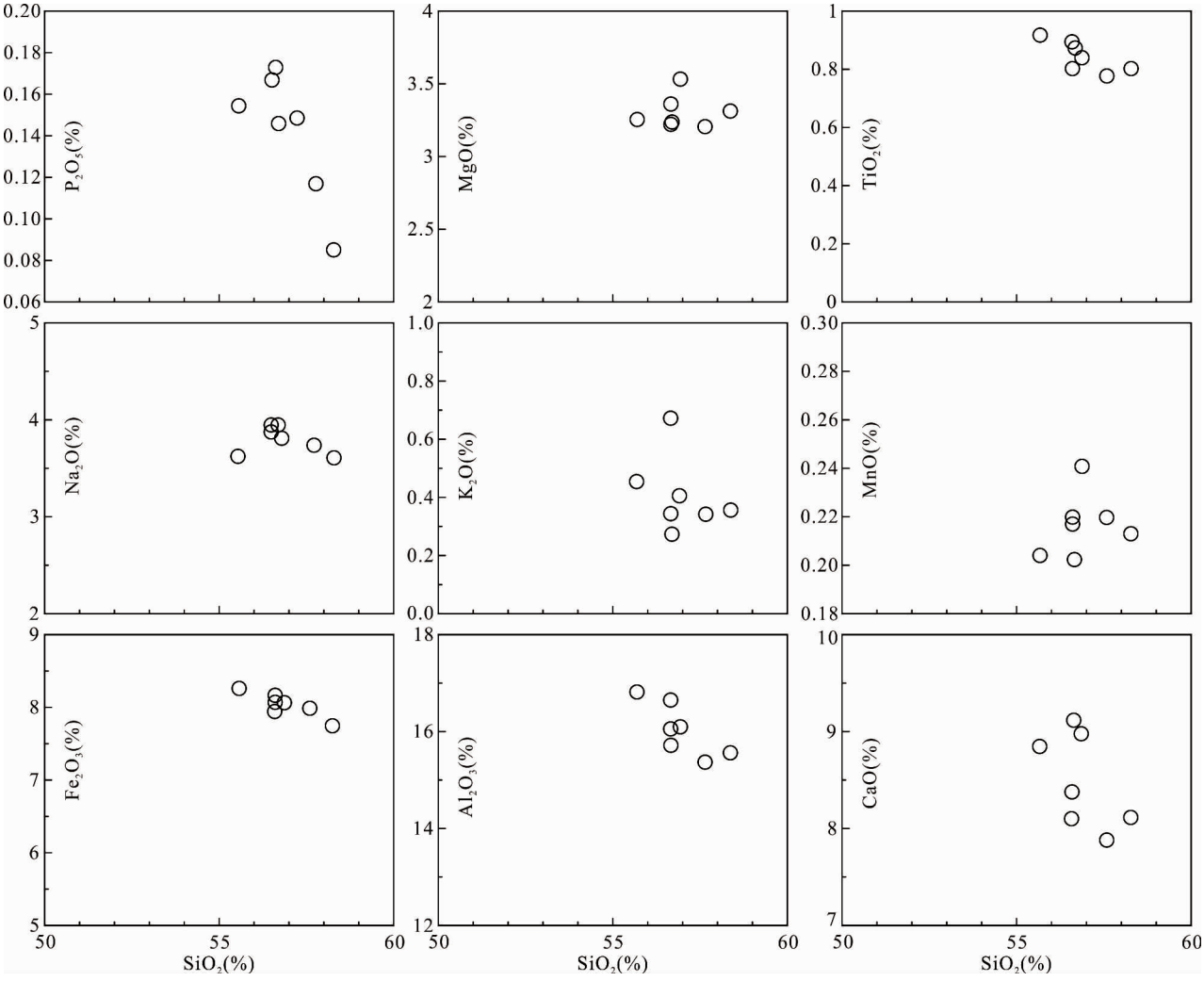


图 6 改则格列戈阿尔辉长岩 Harker 图解

Fig. 6 Harker diagram of the Gelegear gabbro in Gaize

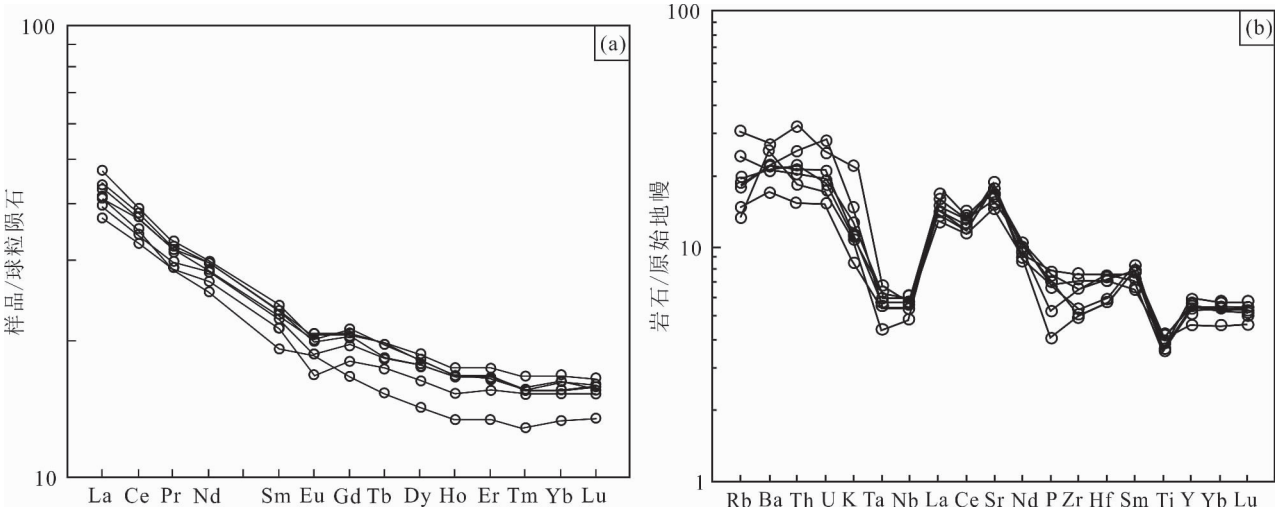


图 7 西藏改则格列戈阿尔辉长岩稀土元素球粒陨石标准化图解(a)和微量元素原始地幔蛛网图(b)

Fig. 7 Chondrite-normalized REE patterns (a) and Primitive mantle-normalized trace elements patterns (b) of the Gelegear gabbro in Gaize

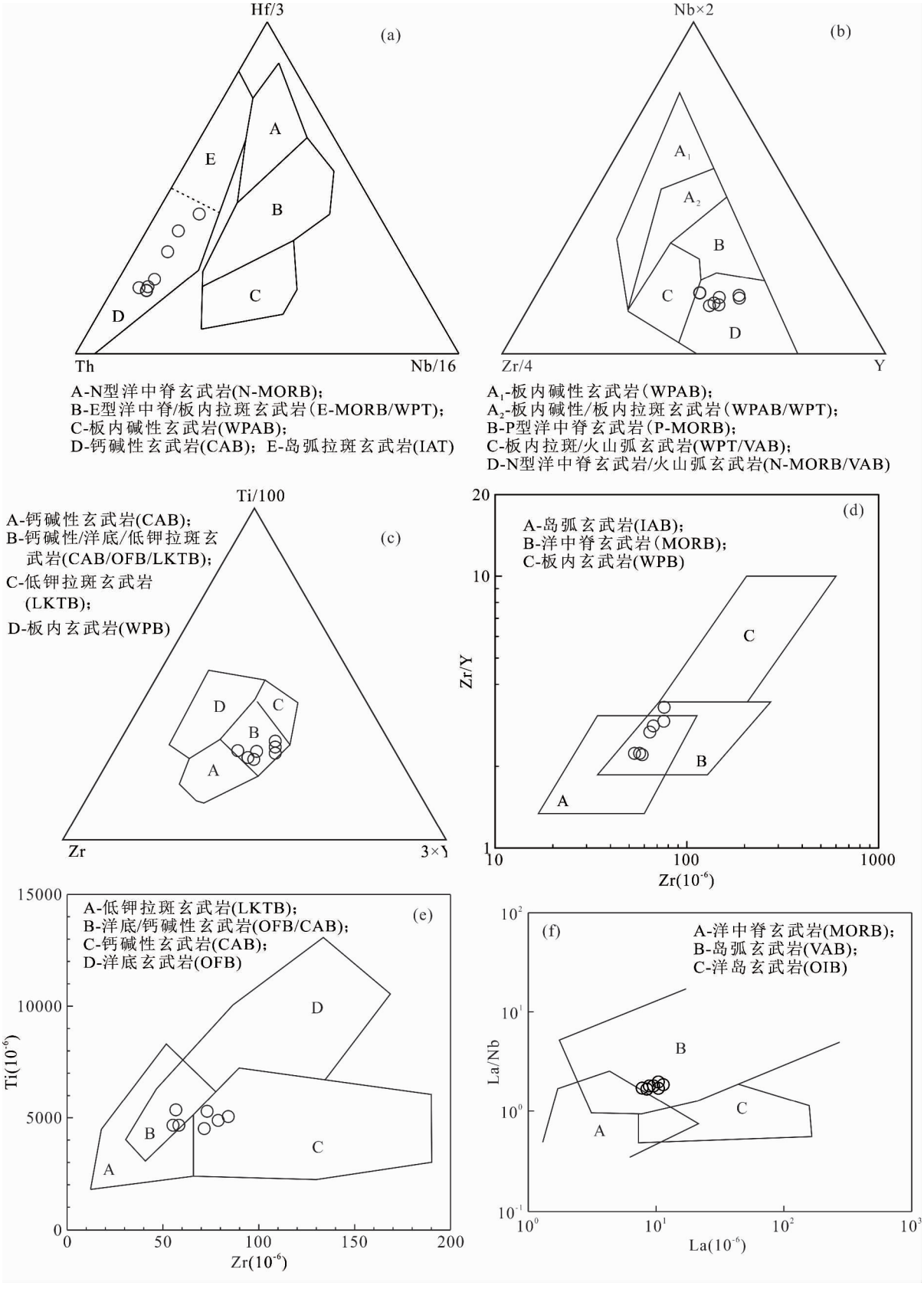


图 8 改则格列戈阿尔辉长岩构造环境判别图

Fig. 8 Diagrams of tectonic environment for the Gelegear gabbro in Gaize

底图引自/after: Meschede,1986;Meschede,1986;Pearce,1973

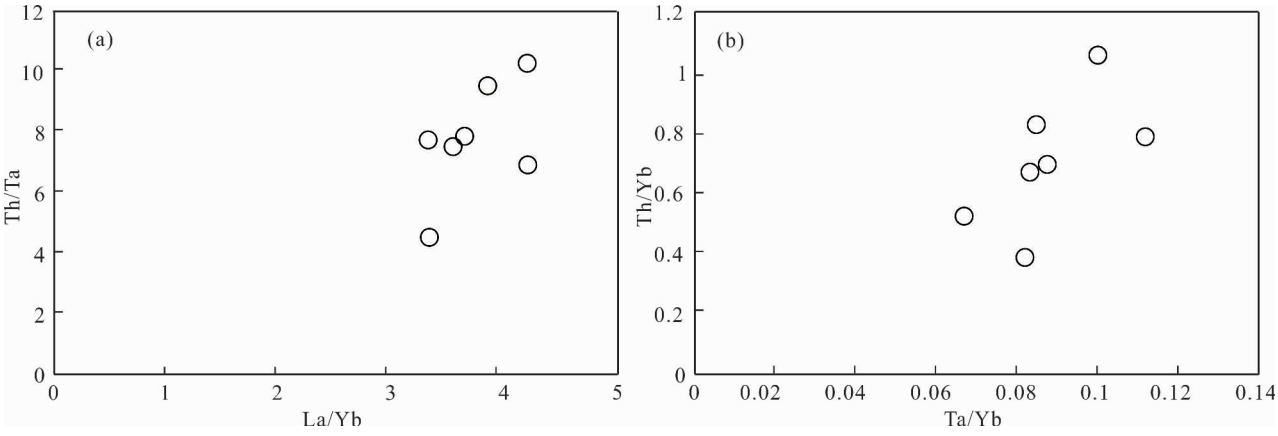


图 9 改则格列戈阿尔辉长岩同化混染判别图解:La/Yb—Th/Ta 和 Ta/Yb—Th/Yb

Fig. 9 Discrimination diagrams of assimilation and contamination of the Gelegear gabbro in Gaize: La/Yb—Th/Ta and Ta/Yb—Th/Yb

型地幔 Ce/Pb = 25 ± 5(Hofmann et al.,1986)。格列戈阿尔辉长岩体中 Ce/Pb 比值在 7.16 ~ 8.16 之间,明确显示了岩体受到同化混染作用;Nb/U 比值可作为判别地壳混染标志之一(Taylor et al.,1985,邓晋福等,2015b),洋中脊玄武岩和洋岛玄武岩 Nb/U 比值为 47 ± 10,而大陆地壳和原始地幔 Nb/U 平均值分别为 8.93 和 33.59,格列戈阿尔辉长岩 Nb/U 比值在 6.56 ~ 12.00 之间,远离原始地幔平均值,接近大陆地壳,反映在俯冲消减环境中辉长岩岩浆源在上升过程中有陆壳物质的混入,岩石成因与俯冲作用相关。从 La/Yb—Th/Ta、Ta/Yb—Th/Yb 图解(图 9)可以看出,格列戈阿尔岩体中岩石不同元素比值之间具有一定的正相关性,可能暗示岩浆演化过程中发生了不同程度的同化混染作用。Neal 等提出可以用 $(La)_{PM}/(Nb)_{PM}$ 与 $(Th)_{PM}/(Ta)_{PM}$ 图解(图 10)来区分上地壳和下地壳物质对原始岩浆的混染作用(Neal et al.,2002,姜常义等,2015),其中,$(*)_{PM}$ 为元素含量的原始地幔标准化后的值。图上可知,岩体遭受了上地壳物质的混染。因此,格列戈阿尔辉长岩原生岩浆为被俯冲改造的岩石圈地幔源岩浆。同时,岩浆在演化过程中一定程度上遭受了上地壳物质的同化混染,并经历一定程度的结晶分异作用。

5.3　班公湖—怒江缝合带构造演化

前人分别对班公湖 MOR 型蛇绿岩和东巧蛇绿岩的地幔橄榄岩进行测年工作,并得到 254 ± 28Ma(黄启帅等,2012)和 251 ± 65Ma(Shi Rendeng et al.,2012),两个年龄可以代表班公湖—怒江洋的初始裂解时间。传统的拉萨地块和羌塘地块之间存在两个洋盆:班怒洋和 Slainajap 洋。需要注意的是,雅江缝合带和班公湖—怒江缝合带之间也存在一条蛇绿岩带:狮泉河—拉果错—阿索—永珠—纳木错—嘉黎—波密蛇绿岩带(简称 Slainajap 带),在弧间裂谷基础上又发展演化出一系列藕断丝连的小洋盆,称之为 Slainajap 洋(潘桂棠等,2006),而北拉萨地块则位于班公湖—怒江缝合带和 Slainajap 蛇绿岩带之间,且 Slainajap 洋盆和班公湖—怒江洋盆发展都是东早西晚,可能与班怒洋的演化存在一定的联系性(王保弟等,2007,付佳俊等,2015)。因此,晚三叠世以前,特提斯域已经形成多岛洋格局(潘桂棠等,2006,王保弟等,2007)(图 11a)。

新特提斯洋向北俯冲产生的岩浆活动在冈底斯

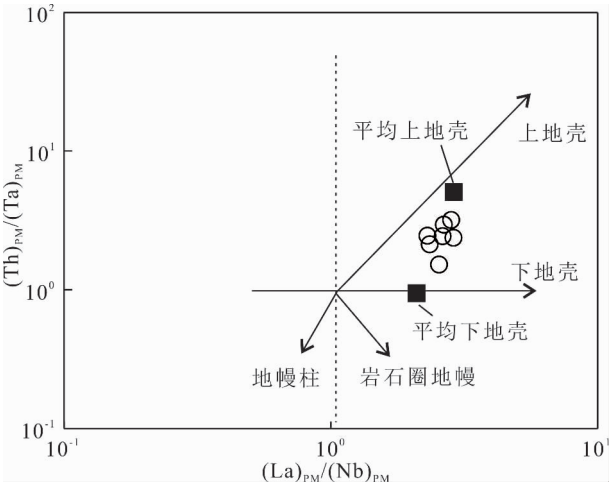


图 10 改则格列戈阿尔辉长岩 $(La)_{PM}/(Nb)_{PM}$ 图解

Fig. 10 Diagrams of $(La)_{PM}/(Nb)_{PM}$ for the Gelegear gabbro in Gaize

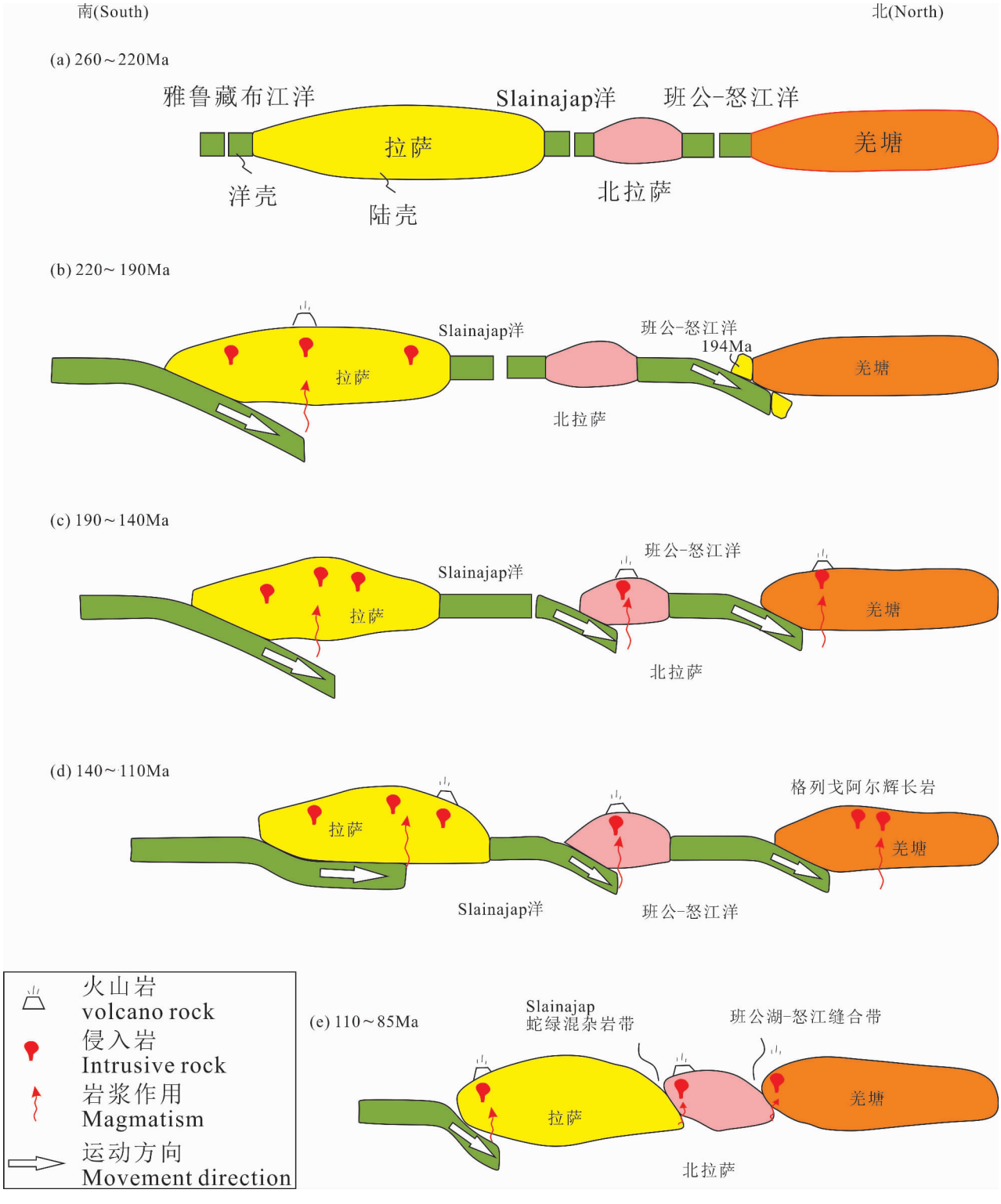


图 11 班公—怒江洋构造演化(据付佳俊等,2015 和 Zhang Yuxiu et al. ,2016 修改)

Fig. 11 Tectonic evolution of the Bangong—Nujiang Ocean(after Fu Jiajun et al. ,2015& and Zhang Yuxiu et al. ,2016)

弧中大量存在,多为中侏罗世:和钟铧等在拉萨地块南部黑云角闪花岗岩中获取角闪石的$^{40}Ar/^{39}Ar$年龄为 215Ma,被认为是洋壳俯冲作用产物(和钟铧等,2006);李才等在南木林县附近的巨斑状花岗闪长岩中获取 217Ma 的单颗锆石 U-Pb 年龄(李才等,2003),以上两者是目前拉萨地块中发现的代表岛

弧岩浆作用的最老年龄。随着俯冲作用的持续,拉萨地块南部和中部后来又有大量早侏罗世岛弧型花岗岩和火山岩的发现:拉萨地块早侏罗世(188Ma)黑云母花岗岩(Chu Meifei et al.,2009);谢通门县雄村铜金矿床的(195Ma、179Ma、175Ma)侵入岩(曲晓明等,2007);叶巴组(182~174Ma)的火山岩(董彦辉等,2006;耿全如等,2006)。前人在班公湖—怒江构造带改则段中发现榴辉岩,并通过角闪石$^{40}Ar/^{39}Ar$测年得出榴辉岩折返时间为 194Ma(Zhang Yuxiu et al.,2016)因此说明班公湖—怒江洋至少在早侏罗世已经发生俯冲作用,而 Slainajap 洋开始俯冲时间可能与班怒洋不一致(图 11b)。

Slainajap 洋向北俯冲作用在中侏罗世已经开始:拉果错蛇绿岩中斜长花岗岩年龄为 166Ma(张玉修,2007);北冈底斯带中接奴群为中晚侏罗世火山沉积地层(朱弟成等,2008)。中晚侏罗世时期,班公湖—怒江洋向北俯冲作用引起的岩浆活动在羌塘南缘也有记录(Li Jinxiang et al.,2014,杜道德等,2011),见图 11c。

早白垩世(140~100Ma),雅江缝合带继续俯冲,拉萨地块中部岩浆活动较为发育。北拉萨地块广泛分布早白垩世岩浆活动记录(去申拉组、多尼组及早白垩世的花岗岩),可能是对 Slainajap 洋盆向北俯冲作用响应的结果。同时,在羌塘地块南缘发育着大量的该期岩浆活动,如热那错地区 110Ma 的流纹岩(Kapp et al.,2005)、多不杂富金斑岩铜矿中 121±1.9Ma 的花岗闪长岩(李金祥等,2008)、班公湖—怒江缝合带两侧的 123.75±0.92Ma 的仲岗火山岩(付佳俊等,2015)等,这些岩浆作用都可能是班公湖—怒江洋向北俯冲的产物(图 11d)。

雅江缝合带在晚白垩世(图 11e)向拉萨地块俯冲,在拉萨地块中又有一次大规模岩浆活动记录(管琪等,2010;付佳俊等,2015)。笔者所在项目组在羌塘南缘去申拉组火山岩中获取早白垩世晚期(106.0±0.8 Ma 和 106.0±0.7 Ma)年龄,代表改则地区拉萨地块和羌塘地块碰撞时间(待发表);曲晓明等在拉萨地块中部日阿铜矿区发现一套 90~87Ma 的双峰式斑岩,认为是碰撞后伸展环境下的岩浆产物(曲晓明等 2006),说明拉萨地块与羌塘地块发生碰撞时间应该在该时期,此时 Slainajap 洋和班公湖—怒江洋已经闭合。班公湖—怒江洋盆在晚白垩世早期已经闭合。

6　结论

(1)格列戈阿尔辉长岩 LA-ICP-MS 锆石 U-Pb 年龄为 122.9±1.6Ma,代表其形成时代为早白垩世晚期。地球化学特征显示该岩体属于亚碱性辉长岩,具有轻稀土富集,弱的 Eu 负异常,富集 LILE,亏损 HFES。

(2)格列戈阿尔辉长岩是被俯冲改造的幔源岩浆经历一定程度的分离结晶作用形成的,岩浆演化过程中遭受了上地壳物质的同化混染。岩体形成于岛弧环境,为班公—怒江洋向北俯冲的产物。

(3)格列戈阿尔辉长岩所代表的岩浆活动表明至少在 122.9±1.6Ma 期间班公—怒江洋盆正在向北俯冲。结合区域资料,研究区班公—怒江洋盆闭合时间应介于 110~85Ma 之间。

致谢:感谢南京大学周国庆教授和匿名终审专家提出宝贵的意见和帮助!锆石测年工作得到了中国地质科学院矿产资源研究所重点实验室侯可军博士的帮助!同时,对一起参加野外工作的曾江、纪国忠、余浩等同志表示真诚的感谢!

参　考　文　献　/　References

(The literature whose publishing year followed by a "**&**" is in Chinese with English abstract; the literature whose publishing year followed by a "#" is in Chinese without English abstract)

杜德道,曲晓明,王根厚,辛洪波,刘治博. 2011. 西藏班公湖—怒江缝合带西段中特提斯洋盆的双向俯冲:来自岛弧型花岗岩锆石 U-Pb 年龄和元素地球化学的证据. 岩石学报, 27(7):1993~2002.

邓晋福,刘翠,冯艳芳,肖庆辉,狄永军,苏尚国,赵国春,段培新,戴蒙. 2015a. 关于火成岩常用图解的正确使用:讨论与建议. 地质论评, 61(4):717~734.

邓晋福,冯艳芳,狄永军,刘翠,肖庆辉,苏尚国,赵国春,孟斐,马帅,姚图. 2015b. 岩浆弧火成岩构造组合与洋陆转换. 地质论评, 61(3):473~484.

董彦辉,许继峰,曾庆高,王强,毛国政,李杰. 2006. 存在比桑日群弧火山岩更早的新特提斯洋俯冲记录么? 岩石学报,22(3):661~668.

杜德道,曲晓明,王根厚,辛洪波,刘治博. 2011. 西藏班公湖—怒江缝合带西段中特提斯洋盆的双向俯冲:来自岛弧型花岗岩锆石 U-Pb 年龄和元素地球化学的证据. 岩石学报,27(7):1993~2002.

付佳俊,丁林,许强,蔡福龙,岳雅慧,郭钰. 2015. 西藏改则洞错地区白垩纪火山岩锆石 U-Pb 年代学、Hf 同位素组成及对班公—怒江洋俯冲闭合的制约. 地质科学,50(1):182~202.

耿全如,潘桂堂,王立全,朱弟成,廖忠礼. 2006. 西藏冈底斯带叶巴组火山岩同位素地质年代. 沉积与特提斯地质,26(1):1~7.

管琪,朱弟成,赵志丹,张亮亮,刘敏,李小伟,于枫,莫宣学. 2010. 西藏南部冈底斯带东段晚白垩世埃达克岩:新特提斯洋脊俯冲的产物. 岩石学报,26(7):2165~2179.

和钟铧,杨德明,郑常青,王天武. 2006**&**. 冈底斯带门巴花岗岩同位素测年及其对特提斯洋俯冲时代的约束. 地质论评,52(1):100~106.

侯可军,李延河,田有荣. 2009. LA-MC-ICP-MS 锆石微区原位 U-Pb 定年技术. 矿床地质,28(4):481~492.

黄启帅,史仁灯,丁炳华,刘德亮,张晓冉,樊帅权,支霞臣. 2012. 班公湖 MOR 型蛇绿岩 Re-Os 同位素特征对班公湖—怒江特提斯洋裂解时间的制约. 岩石矿物学杂志,31(4):465 ~ 478.

姜常义,穆艳梅,赵晓宁,白开寅,张虹波. 2001. 塔里木板块北缘活动陆缘型侵入岩带的岩石学与地球化学. 中国区域地质,20(2):158 ~ 163.

姜常义,王子玺,杜玮,王梦玺. 2015&. 柴达木地块北缘南北沟岩体地球化学特征及成矿前景. 地球科学与环境学报,37(1):12 ~ 23.

李才,王天武,李惠民,曾庆高. 2003. 冈底斯地区发现印支期巨斑花岗闪长岩—古冈底斯造山存在证据. 地质通报,22(5):364 ~ 366.

李金祥,李光明,秦克章,肖波. 2008. 班公湖带多不杂富金斑岩铜矿床斑岩—火山岩的地球化学特征与时代:对成矿构造背景的制约. 岩石学报,24(3):531 ~ 543.

潘桂棠,莫宣学,侯增谦,朱弟成,王立全,李光明,赵志丹,耿全如,廖忠礼. 2006. 冈底斯造山带的时空结构及演化. 岩石学报,22(3):521 ~ 533.

秦川,李智武,朱利东,张玉修,杨文光,黄瑞. 2015. 西藏羌塘地体南缘改则嘎布扎花岗闪长岩侵位时代、成因及其地质意义. 中国地质,42(1):105 ~ 117.

曲晓明,辛洪波,徐文艺,杨竹森,李振清. 2006. 藏西措勤含铜双峰岩系的发现及其意义. 岩石学报,22(3):707 ~ 716.

曲晓明,辛洪波,徐文艺. 2007. 西藏雄村特大型铜金矿床容矿火山岩成因及其对成矿的贡献. 地质学报,81(7):964 ~ 971.

曲晓明,王瑞江,辛洪波,赵元艺,樊兴涛. 2009. 西藏西部与班公湖特提斯洋盆俯冲相关的火成岩年代学和地球化学. 地球化学,38(6):523 ~ 535.

田亚洲,杨经绥,刘飞,赵一玉,冯光英,牛晓露,张岚,高健. 2014. 新疆布鲁斯台辉长岩岩石学特征及对南天山洋俯冲时限的制约. 岩石学报,30(8):2363 ~ 2380.

王保弟,许继峰,曾庆高,康志强,陈建林,董彦辉. 2007. 西藏改则地区拉果错蛇绿岩地球化学特征及成因. 岩石学报,23(6):1521 ~ 1530.

姚晓峰,唐菊兴,李志军,邓世林,丁帅,胡正华,张志. 2013. 班公湖—怒江带西段尕尔穷矽卡岩型铜金矿含矿母岩成岩时代的重新厘定及其地质意义. 地质论评,29(1):193 ~ 200.

尹光侯,侯世云. 1998. 西藏碧土地区怒江缝合带基本特征与演化. 中国区域地质,17(3):246 ~ 254.

张旗,周国庆. 2001. 中国蛇绿岩. 北京:科学出版社,1 ~ 176.

张玉修. 2007. 班公湖—怒江缝合带中西段构造演化(博士论文). 广州:中国科学院广州地球化学研究所. 1 ~ 268.

赵元艺,刘妍,崔玉斌,吕立娜,宋亮,曲晓明. 2010. 西藏班公湖—怒江成矿带与邻区锢矿化带的发现及意义. 地质论评,56(4):568 ~ 578.

朱弟成,潘桂棠,莫宣学,王立全,廖忠礼,赵志丹,董国臣,周长勇. 2006. 冈底斯中北部晚侏罗世—早白垩世地球动力学环境:火山岩约束. 岩石学报,22(3):534 ~ 546.

朱弟成,潘桂堂,王立全,莫宣学,赵志丹,周长勇,廖忠礼,董国臣,袁四化. 2008. 西藏冈底斯带侏罗纪岩浆作用的时空分布及构造环境. 地质通报,27(4):458 ~ 468.

左祖发,罗春林,王会敏,刘邦秀,刘春根,徐喆. 2015. 赣南横市地区基性岩墙 LA-ICP-MS 锆石 U-Pb 年龄、地球化学特征及其地质意义. 地质论评,61(6):1417 ~ 1428.

Atherton M P, Petford N. 1993. Generation of sodium-rich magmas from newly underplated basaltic crust. Letters to Nature, 362(6416): 145 ~ 146.

Chu Meifei, Chung Sunlin, Song Biao, Liu Dunyi, O'Reilly S Y, Pearson N J, Ji Jianqing, Wen Dajen 2009. Zircon U-Pb and Hf isotope constraints on the Mesozoic tectonic and crustal evolution of southern Tibet. Geology, 34(9): 745 ~ 748.

Deng Jinfu, Liu Cui, Feng Yanfang, Xiao Qinghui, Di Yongjun, Su Shangguo, Zhao Guochun, Duan Peixin, Dai Meng. 2015a. On the Correct Application in the Common Igneous Petrological Diagrams: Discussion and Suggestion. Geological Review, 61(4): 717 ~ 734.

Deng Jinfu, Feng Yanfang, Di Yongjun, Liu Cui, Xiao Qinghui, Su Shangguo, Zhao Guochun, Meng Fei, Ma Shuai, Yao Tu. 2015b. Magmatic Arc and Ocean—Continent Transition: Discussion. Geological Review, 61(3): 473 ~ 484.

Dong Yanhui, Xu Jifeng, Zeng Qinggao, Wang Qiang, Mao Guozheng, Li Jie. 2006&. Is There a Neo-Tethys' Subduction Record Earlier than arc volcanic rocks in the Sangri Group? Acta Petrologica Sinica, 22(3): 661 ~ 668.

Du Dedao, Qu Xiaoming, Wang Genhou, Xin Hongbin, Liu Zhibo. 2011&. Bidirectional subduction of the Middle Tethys oceanic basin in the west segment of Bangonghu—Nujiang suture, Tibet: Evidence from zircon U-Pb LA-ICP-MS dating and petrogeochemistry of arc granites. Acta Petrologica Sinica, 27 (7): 1993 ~ 2002.

Fu Jiajun, Ding Lin, Xu Qqiang, Cai Fulong, Yue Yahui, Guo Yu. 2015&. Zircon U-Pb geochronology and Hf isotopic composition of the Cretaceous volcanic rocks and constraint of the collision age of Bangong—Nujiang suture zone in Dongco area, Gaize, Tibet. Chinese Journal of Geology, 50(1): 182 ~ 202.

Geng Quanru, Pan Guitang, Wang Liquan, Zhu Dicheng, Liao Zhongli. 2006&. Isotopic geochronology of the volcanic rocks from the Yeba Formation in the Gangdise zone, Xizang. Sedimentary Geology and Tethyan Geology, 26(1): 1 ~ 7.

Guan Qi, Zhu Dicheng, Zhao Zhidan, Zhang Liangliang, Liu Min, Li Xiaowei, Yu Feng, Mo Xuanxue. 2010&. Late Cretaceous adakites in the eastern segnent of the Gangdese Belt, southern Tibet: Products of Neo-Tethyan ridge subduction. Acta Petroloica Sinica, 26(7): 2165 ~ 2179.

He Zhonghua, Yang Deming, Zheng Changqing, Wang Tianwu. 2006&. Isotopic dating of the Mamba granitoid in the Gangdise tectonic belt and its constraint on the subduction time of the Neotethys. Geological Review, 52(1): 100 ~ 106.

Hou Kejun, Li Yanhe, Tian Yourong. 2009&. In situ U-Pb zircon dating using laser ablation-multiion counting-ICP-MS. Mineral Deposits, 28(4): 481 ~ 492.

Huang Qishuai, Shi Rendeng, Ding Binghua, Liu Deliang, Zhang Xiaoran, Fan Shuaiquan, Zhi Xiachen. 2012&. Re-Os isotopic evidence of MOR-type ophiolite from the Bangong Co for the opening of Bangong—Nujiang Tethys Ocean. Acta Petrologica et Mineralogica, 31(4): 465 ~ 478.

Jakes P, White A R. 1972. Major and trace element abudances in volcanic rocks of orogenic areas. Geological Society of America Bulletin, 83(1): 29 ~ 40.

Jiang Changyi, Mu Yanmei, Zhao Xiaoning, Bai Kaiyan, Zhang Hongbo. 2001&. Petrology and geochemistry of an active continental margin intrusive rock belt on the northern margin of the Tarim plate. Regional Geology of China, 20(2): 158 ~ 163.

Jiang Changyi, Wang Zixi, Du Wei, Wang Mengxi. 2015&. Geochemical Characteristics of Nanbeigou Intrusion in the Northern Margin of Qaidam Massif and Its Prospecting Potential. Journal of Earch Sciences and Environment, 37(1): 12 ~ 23.

Kapp P, Murphy M A, Yin A, Mark Harrison. 2003. Mesozoic and

Cenozoic tectonic evolution of the Shiquanhe area of western Tibet. Tectonics,22(4):1 ~ 24.

Kapp P, Yin A, Harrison T M. 2005. Cretaceous—Tertiary shortening, basin development, and volcanism in central Tibet. Geological Society of America Bulletin,117(7):865 ~ 878.

Li Cai, Wang Tianwu, Li Huimin, Zeng Qinggao. 2003&. Discovery of Indosinian megaporphyritic granodiorite in the Gangdise area: evidence for the existence of Paleo-Gangdise. Geological Bulletin of China,22(5):364 ~ 366.

Li Jinxiang, Li Guangming, Qin Kezhang, Xiao Bo. 2008&. Geochemistry of porphyries and volcanic rocks and ore-forming geochronology of Duobuza gold-rich porphyry copper deposit in Bangonghu belt, Tibet: Constraints on metailogenic tectonic settings. Acta Petrologica Sinica,24(3):531 ~ 543.

Li J X, Qin K Z, Li G M et al. 2014. Geochronology, geochemistry, and zircon Hf isotopic compositions of Mesozoic intermediate—felsic instrusions in central Tibet: Petrogenetic and tectonic implications. Lithos,198(1):77 ~ 91.

Mechede M. 1986. A method of discriminating between different types of mid-ocean ridge basalts and continental tholeiites with the Nb—Zr—Y diagram. Chemical Geology,56(3 ~ 4):207 ~ 218.

Neal C R, Mahoney J J, Chazey W J. 2002. Mantle Sources and the Highly Variable Role of Continental Lithosphere in Basalt Petrogenesis of the Kerguelen Plateau and Broken Ridge LIP: Results from ODP Leg 183. Journal of Petrology,43(7):1177 ~ 1205.

Pan Guitang, Mo Xuanxue, Zhu Dicheng, Wang Liquan, Li Guangming, Zhao Zhidan, Geng Qquanru, Liao Zhongli. 2006&. Spatial—temporal framework of the Gangdese Orogenic Belt and its evolution. Acta Petrologica Sinica,22(3):521 ~ 533.

Pearce J A, Cann J R. 1973. Tectonic setting of basic volcanic rocks determined using trace element analyses. Earth and Planetary Science Letters,19(2):290 ~ 300.

Qin Chuan, Li Zhiwu, Zhu Lidong, Zhang Yuxiu, Yang Wenguang, Huang Rui. 2015&. The emplacement epoch, petrogenesis and geological significance of Gabuzha granodiorite at the southern edge of Qiangtang, Tibet. Geology in China,42(1):105 ~ 117.

Qu Xiaoming, Xin Hongbo, Xu Wenyi, Yang Zhusen, Li Zhenqing. 2006&. Discovery and singificance of copper-bearing bimodal rock series in Coqin area of Tibet. Acta Petrologica Sinica,22(3):707 ~ 716.

Qu Xiaoming, Xin Hongba, Xu Wenyi. 2007&. Petrogenesis of the Ore-Hosting Volcanic Rocks and Their Contribution to Mineralization in Xiongcun Superlarge Cu—Au Deposit, Tibet. Acta Geologica Sinica,81(7):964 ~ 971.

Qu Xiaoming, Wang Ruijiang, Xin Hongbo, Zhao Yuanyi, Fan Xingtao. 2009&. Geochronology and geochemistry of igneous rocks related to the subduction of the Tethys oceanic plate along the Bangong Lake arc zone, the western Tibetan Plateau. Geochimica,38(6):523 ~ 535.

Shi Rendeng, Griffin W L, O'Reily S Y. 2012. Melt—mantle mixing produces podiform chromite deposites in ophiolites: Implications of Re-Os systematics in the Dongqiao Neo-tethyan ophiolite, northern Tibet. Gangwana Research,21(1):194 ~ 206.

Sun S S, McDonough W F. 1989. Chemical and isotopic systematics of oceanic basalts: Implications for mantle composition and processes. Geological Society London Special Publication,42(1):313 ~ 345.

Taylor, S R, McLennan S M. 1985. The continental crust: its composition and evolution. London: Blackwell,57 ~ 72.

Tian Yazhou, Yang Jingsui, Liu Fei, Zhao Yiyu, Feng Guangying, Niu Xiaolu, Zhang Lan, Gao Jian. 2014&. Petrological characteristics of Bulusitai gabbro and its constraint to the time of South Tianshan ocean subduction. Acta Petrologica Sinica,30(8):2363 ~ 2380.

Wang Baodi, Xu Jifeng, Zeng Qinggao, Kang Zhiqiang, Chen Jianlin, Dong Yanhui. 2007&. Geochemistry and genesis of Lhaguo Tso ophiolite in south of Gerze area, Center Tibet. Acta Petrologica Sinica, 23(6):1521 ~ 1530.

Wilson M. 1989. Igneous Petrigenisis. London: Unwin Hyman,1 ~ 466.

Yao Xiaofeng, Tang Juxing, Li Zhijun, Deng Shilin, Ding Shuai, Hu Zhenghua, Zhang Zhi. 2013&. The Redefinition of the Ore-forming Porphyry's Age in Gaerqiong Skarn-type Gold—Copper Deposit, Western Bangong Lake—Nujiang River Metallogenic Belt, Xizang (Tibet). Geological Review,29(1):193 ~ 200.

Yin Guanghou, Hou Shiyun. 1998&. Basic Features and Evolution of the Nujiang River Suture Zone in the Bitu Area, Tibet. Regional Geology of China,17(3):246 ~ 254.

Zhang K J, Zhang Y X, Li B, Zhong L F. 2007. Nd isotopes of siliciclastic rocks from Tibet, western China: Constraints on the pre-Cenozoic tectonic evolution. Earth and Planetary Science Letters, 256: 604 ~ 616.

Zhang K J, Zhang Y X, Tang X C, Xie Y W, Sha S L, Peng, X J. 2008. First report of eclogites from central Tibet, China: evidence for ultradeep continental subduction prior to the Cenozoic India—Asian collision. Terra Nova,20:302 ~ 308.

Zhang K J, Zhang Y X, Tang X C, Xia B. 2012. Late Mesozoic tectonic evolution and growth of the Tibetan plateau prior to the Indo—Asian collision. Earth Science-Reviews 114:236 ~ 249.

Zhang K J, Zhang Y X, Xia, B D, He Y B. 2006. Temporal variations of the Mesozoic sandstone composition in the Qiangtang block, northern Tibet (China): Implications for provenance and tectonic setting. Journal of Sedimentary Research 76:1035 ~ 1048.

Zhang Qi, Zhou Guoqing. 2001#. Chinese Ophiolite. Beijing: Science Press,1 ~ 176.

Zhang Y X, Li Z W, Zhu L D, Zhang K J, Yang W G, Jin X. 2015. Newly discovered eclogites from the Bangong Meso-Tethyan suture zone (Gaize, central Tibet, western China): Mineralogy, geochemistry, geochronology, and tectonic implications. International Geology Review,58(5):574 ~ 587.

Zhang Yuxiu. 2007&. Tectonic Evolution of the Middle—Western Bangong—Nujiang Suture, Tibet (PhD Thesis). Guangzhou: Guangzhou Institute of Geochemistry, Chinese Academy of Sciences. 1 ~ 268.

Zhao Yuanyi, Liu Yan, Cui Yubin, Lv Lina, Song Liang, Qu Xiaoming. 2010&. Discovery and Significant of Indium Mineralization Belt in Bangong Lake—Nujiang River Metallogenic Belt and Adjacent Regions in Tibet. Geological Review,56(4):568 ~ 578.

Zhu Dicheng, Pan Guitang, Mo Xuanxue, Wang Liquan, Liao Zhongli, Zhao Zzhidan, Dong Guochen, Zhou Changyong. 2006&. Late Jurassic—Early Cretaceous geodynamic setting in middle—northern Gangdese: New insights from volcanic rocks. Acta Petrologica Sinica,22(3):534 ~ 546.

Zhu Dicheng, Pan Guitang, Wang Liquan, Mo Xuanxue, Zhao Zhidan, Zhou Changyong, Liao Zhongli, Dong Guochen, Yuan Sihua. 2008&. Spatial—temporal distribution and tectonic setting of Jurassic magmatism in the Gangdise belt, Tibet, China. Geological Bulletin of China,27(4):458 ~ 468.

Zuo Zufa, Luo Chunlin, Wang Huimin, Liu Bangxiu, Liu Chungeng, Xu

Zhe. 2015&. LA-ICP-MS Zircon U-Pb Ages, Geological Characteristics of Silurian Basic Dykes in Hengshi Area, Southern Jiangxi, and Their Geological Significances. Geological Review, 61(6): 1417 ~ 1428.

LA-ICP-MS Zircon U-Pb Dating, Geochemistry and Tectonic Implications of the Gelegear Gabrro at the Sourthern Edge of Qiangtang Terrance, Gaize, Xizang(Tibet)

TAO Gang[1)], LI Zhiwu[1,2)], ZHU Lidong[1)], ZHANG Yuxiu[3)], YANG Wenguang[1)], CHEN Shun[4)], XIE Long[1)], YANG Zhen[1)], HE Yuan[1)], LIU He[1)], LI Chao[1)]

1) *Institute of Sedimentary Geology, Chengdu University of Technology, Chengdu*, 610059;

2) *State Key Laboratory of Oil and Gas Reservoir Geology and Exploitation, Chengdu University of Technology, Chengdu*, 610059;

3) *University of Chinese Academy of Sciences, Beijing*, 100049;

4) 282 *Group of Bureau of Geology for Nuclear Industry, Deyang, Sichuan*, 618000

Abstract: Bangong Co—Nujiang River (Bangong Lake—Nujiang River) suture is one of the largest sutures in the Qinghai—Xizang (Tibet) Plateau and it is situated between the Qiangtang terrance and the Lhasa terrance.

With its complex tectonic settings, there are existed many disputes on the Bangong Co—Nujiang River suture, especially in Gaize area, which are mainly about two basic and key issues, which restrict our researches on the geological settings and the evolution of the Xizang. They are the polarity of subduction and the timing of opening.

Based on the petrology, geochemistry and chronology of the Gelegear gabbro in Gaize area, we focus on its formation age, petrogenesis, tectonic settings and the evolution process of the subduction to closing.

The gabbro sample separation and target preparation of zircons was carried out at the Lab Test Center of the Hebei Institute's Regional Geology & Mineral Survey. The samples were processed by contaminant free crushing. The zircon grains were obtained by selection under a binocular eyepiece after magnetic and electrical separation. Representative zircon grains were then selected for target preparation, and transmission and reflected light photography was used to investigate the zircons by cathode luminescence. Zircon U-Pb dating was performed by LA-ICP-MS at the Mineral Resource Institute of the Chinese Academy of Geological Sciences, with a Newwave UP 213 laser ablation system and the FinniganNeptune; U, Th, Pb, and other elements had an integration time of 20s. Data processing was performed using Isoplot 3.0 software and the data was with a high concordance degree was eliminated.

The major elements testing is in School of Geosciences and Info-Physics, Central South University. It used powder direct compression with instrument of ZSX Primus II X-ray fluorescene.

Spectrometer with analytical precision less than 1%. Trace elements testing is completed in Institute of Tibetan Plateau Research Chinese Academy of Sciences with instrument of X series ICP-MS. The testing samples are preprocessed by using acid dissolution.

The LA-ICP-MS dating indicates that the babbro was emplanced at 122.9 ± 1.6Ma. The babbro is formed in the Early Cretaceous. Geochemical data show that the Gabbro consists high content of Al_2O_3 (15.39% ~ 16.83%), low content of TiO_2 (0.78% ~ 0.92%), P_2O_5 (0.09% ~ 0.17%), ($Na_2O + K_2O$ = 3.93% ~ 4.41%). The REE content is between 63.37×10^{-6} and 73.76×10^{-6}, average 68.84×10^{-6}, with $(La/Yb)_N$ ratio of 2.43 ~ 3.09 and δEu of 0.89 ~ 1.03. REE diagram shows rightward incline and week negative Eu abnormity. The gabbro is remarkably characterized by enrich LREE and depleted HREE. The LILE such as Rb, Ba, Th, U is enriched, while HFSE such as Nb, Ta, P, Ti is depleted. The ratios of Nb/Ta and Zr/Hf are sharp beneath that of primitive mantle.

The geochemical characteristics and tectonic discriminations show that the parental magma of gabbro derived probably from the mantle influenced by the subduction. The parental magma is developed by the upper crustal assimilation contamination during the magma evolution and experience a certain extent of separation and

crystallization as well. The Gelegear gabbro formes in an island arc environment related to northward subduction of the Bangong—Nujiang and indicates that during 122.9 ± 1.6Ma, Bangong—Nujiang oceanic basin continues its northward subduction in research area. Combined with regional data, this study concludes that the closure time of Bangong Co—Nujiang River ocean basin was between 110Ma and 85Ma in the Gaize area.

Keywords: Gabrro; Zircon U-Pb dating, Geochemistry; Tectonic Implications; Island Arc; Bangong Co—Nujiang River Suture Zone; Qiang Tang

Acknowledgements: This study was financially supported by Chinese Geological Survey (No. 1212011086065, 12120113033004), the Natural Science Foundation of China (41472209, 41002055) and the the Research Fund for the Doctoral Program of Higher Education (20125122110010). We would like to express our thanks to Professor Zhou Guoqing from Nanjing University and the anonymous reviewer for examining the manuscripts.

First author: TAO Gang, male, born in 1988, a Ph. D. of Paleontology and Stratigraphy, is mainly engaged in the research of regional investigation and the Paleontologic Research. Address: East 3rd Road, Erxianqiao, Chenghua District, Chengdu, 610059. Email: taogang0428@163.com

Corresponding author: LI Zhiwu, male, born in 1976, a professor, is mainly engaged in structural geology and petroleum geology. Email: lizhiwu06@cdut.cn

Manuscript received on: 2016-01-20; Accepted on: 2016-08-12; Edited by: ZHANG Yuxu.

Doi: 10.16509/j.georeview.2016.05.005